

# Realization of a timescale with an accurate optical lattice clock

CHRISTIAN GREBING,\* ALI AL-MASOUDI, SÖREN DÖRSCHER, SEBASTIAN HÄFNER, VLADISLAV GERGINOV, STEFAN WEYERS, BURGHARD LIPPHARDT, FRITZ RIEHLE, UWE STERR, AND CHRISTIAN LISDAT

Physikalisch-Technische Bundesanstalt, Bundesallee 100, 38116 Braunschweig, Germany

\*Corresponding author: christian.grebing@ptb.de

Received 22 February 2016; revised 15 April 2016; accepted 19 April 2016 (Doc. ID 259633); published 25 May 2016

Optical clocks are not only powerful tools for prime fundamental research, but are also deemed for the redefinition of the SI base unit “second,” as they now surpass the performance of cesium atomic clocks in both accuracy and stability by more than an order of magnitude. However, an important obstacle in this transition has so far been the limited reliability of optical clocks, which made a continuous realization of a timescale impractical. In this paper, we demonstrate how this situation can be resolved and show that a timescale based on an optical clock can be established that is superior to one based on even the best cesium fountain clocks. The paper also gives further proof of the international consistency of strontium lattice clocks on the  $10^{-16}$  accuracy level, which is another prerequisite for a change in the definition of the second. © 2016 Optical Society of America

**OCIS codes:** (120.3940) Metrology; (020.1335) Atom optics; (300.6320) Spectroscopy, high-resolution.

<http://dx.doi.org/10.1364/OPTICA.3.000563>

## 1. INTRODUCTION

The international system of units (SI) is the universal base for all measurements and thus constitutes the backbone of natural sciences and engineering. The definitions themselves and their realizations have been adapted over the years to profit from state-of-the-art research results. Important modifications are at hand for the electrical units and the mass, which will be defined through agreed-upon values of fundamental constants [1].

Due to their impressive progress [2–10], optical clocks surpass cesium fountain clocks, which currently realize the SI “second” with lowest uncertainty in terms of stability and accuracy, realizing an unperturbed atomic transition frequency. This has triggered discussions about the need for a redefinition of this unit [11,12]. A first step has been the acknowledgment of suitable optical transitions in neutral atoms and ions as secondary representations of the SI unit “second” by the Comité International des Poids et Mesures (CIPM) [13].

Given the outstanding role of the SI, it is of paramount importance that adaptations must be prepared carefully. Hence, changes will be acceptable only if an obvious candidate is identified, the transition is smooth, and the new approach is practical [11].

While the first point stimulates ongoing research, the second point has already been addressed satisfactorily for strontium optical lattice clocks [3,14] by measurements of the strontium clock transition frequency with today’s best possible accuracy; the results in this paper confirm the previous measurement results. The latter prerequisite, however, has not been achieved so far for the candidate systems, as existing optical clocks have generally

been considered less reliable and thus less suitable for the actual implementation of a practical timescale, which continuously accumulates the atomic seconds.

Timescales provide us with coordinates for the position of events in time, much like a coordinate system does for the positioning in space. In particular, it needs to be realized without interruption to provide a continuous coordinate or to measure time intervals and synchronize distant events.

Today, the Universal Coordinated Timescale (UTC) is post-processed from a weighted monthly average of the time kept by some 500 microwave atomic clocks around the world that are intercompared via satellite links. Additionally, Rapid UTC (UTC<sub>r</sub>) has recently been introduced to provide a timescale with daily updates computed from a subset of the time laboratories contributing to UTC [15]. However, due to the smaller number of clocks involved, UTC<sub>r</sub> is slightly less stable. To obtain time whenever needed, the time laboratories generate local timescales in real-time typically by steering the output frequency of a continuously running flywheel oscillator (Fig. 1), e.g., a hydrogen maser, on a monthly period to stay synchronized with the UTC clock ensemble [16]. Some time laboratories synchronize their flywheel oscillators on an even shorter period to match the frequency of a local primary Cs clock [17].

The origin of the time error of such real-time timescales with respect to an ideal timescale is twofold: First, the accuracy of the local scale unit is limited by imperfections of the atomic reference(s). Even for the best cesium fountain clocks, this error can integrate to about 1 ns after one month. Second, missing

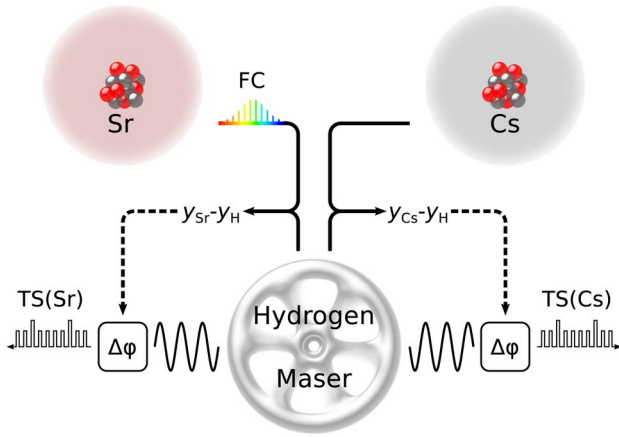


**Fig. 1.** Realization of a timescale TS from a microwave and an optical clock: The Cs clock transition frequency is compared against the maser flywheel frequency. The acquired offset  $y_{\text{Cs}} - y_{\text{H}}$  is used to correct the classical timescale TS(Cs) generated from the maser utilizing a phase stepper ( $\Delta\phi$ ). An equivalent scheme is applicable when referencing the timescale TS(Sr) to an optical frequency standard. For that purpose, the clock laser light is down-converted to the microwave regime using a femtosecond frequency comb (FC) before comparing against the flywheel. Moreover, both maser offsets can be analyzed to yield the Sr clock frequency in SI units.

information from UTC or downtimes of the local atomic reference clock introduce a time error depending on the instability of the flywheel oscillator.

Due to the averaging, UTC is more stable than most local timescales. Thus, in practice the quality of a local timescale is typically assessed by comparison to UTC—which, however, is not an ideal reference. Due to its construction involving many time links, a deviation between the rate of UTC and the “second” of the local fountains can be as large as 0.1 ns/day, which accumulates to a time error of about 3 ns at the end of the month.

If the cesium fountains, which can have insignificant downtimes, are replaced by optical clocks, the time error of local timescales is expected to reduce by more than one order of magnitude (a projected clock uncertainty of  $\lesssim 1 \times 10^{-17}$  corresponds to a time error  $\lesssim 25$  ps after a month)—provided the time error arising from their downtimes is limited to a negligible level—and thus significantly improve the timescale’s predictability. Together with improved time-link technologies [18], a network of optical atomic clocks will allow the generation of a much more stable UTC and thus labeling events in time all over the world more precisely. This would be beneficial for global navigation systems, astrophysics, and fundamental physics.

In this article, we demonstrate how PTB’s strontium lattice clock is now able to maintain a local timescale with a time error of less than 200 ps compared to an ideal reference over about 25 days, or  $7 \times 10^{-17}$  in fractional units. Over this period, the optical clock is allowed to operate with long interruptions (overall clock availability:  $\approx 46\%$ ), and downtimes are bridged by a hydrogen maser flywheel. The distortion of the scale unit due to the use of the flywheel while the clock is offline causes the dominant contribution to the achieved residual time error. However, this shows for the first time, to our knowledge, that optical frequency standards with limited availability can already serve as atomic references to support a local timescale over extended periods, yielding a

long-term performance better than that attributed to the best current microwave clocks even if they are operated free of interruptions. Further improvements of the timescale based on optical clocks are at hand by ever-higher availability of the optical clock. Moreover, the maser-flywheel-assisted Sr data, together with data from our Cs fountains acquired in parallel, enabled us to measure the Sr clock transition frequency with minimum uncertainty. So far, this could only be achieved by operating the clocks for long times and/or by averaging over several of the best fountain clocks [3,14].

## 2. OPTICAL CLOCK OPERATION

The strontium lattice clock was operated during two campaigns, in October 2014 and June 2015, under conditions very similar to those of a previous campaign [14]. A new interrogation laser system [19] improved the estimated optimum fractional frequency instability of the Sr clock, expressed as the Allan deviation  $\sigma$ , to below  $\sigma_{\text{Sr}}(\tau) = 2 \times 10^{-16} / \sqrt{\tau}$  with averaging time  $\tau$  [20].

For best accuracy of the lattice clock, we reduced the duty cycle of the clock interrogation by introducing a dead time, during which the power-dissipating magnetic field coils are switched off. Thus, the reduced power dissipation results in smaller spatial thermal gradients over the experimental apparatus, whereas temporal gradients are suppressed sufficiently by the heat capacity of the apparatus. Gradients limit our knowledge of the AC and DC Stark line shift due to blackbody radiation and thereby cause the greatest uncertainty contribution to our lattice clock. With this reduced duty cycle, our clock still achieved an estimated instability of about  $\sigma_{\text{Sr}}(\tau) = 5 \times 10^{-16} / \sqrt{\tau}$  during the measurement campaign. The clock’s systematic uncertainty  $u_B(\text{Sr})$  of  $1.9 \times 10^{-17}$  has been evaluated similar to [14] and is discussed in detail in Supplement 1. It is at least an order of magnitude smaller than the systematics of PTB’s primary Cs fountain clocks CSF1 and CSF2 [21–24].

From October 6 through 15, 2014, the lattice clock was operated together with CSF2 ( $u_B(\text{CSF2}) = 3.1 \times 10^{-16}$ ) to measure the SI frequency of the Sr clock transition, which we will discuss first. The frequencies of the Cs clock and the Sr lattice clock have been compared via femtosecond frequency combs (FC in Fig. 1). A continuously operated, high-performance hydrogen maser (VREMYA-CH VCH-1003M) used as a flywheel is connected to both clocks, e.g., for the generation of a timescale steered by either the Cs fountain [TS(Cs)] [17] or the lattice clock [TS(Sr)]. During the measurement campaign, the lattice clock was operated over a total uptime of  $T_{\text{Sr}} = 267,000$  s [shown in Fig. 3(a)], together with the almost continuously running fountain clock (availability  $>98\%$ ).

From this simultaneous comparison of the Cs and the Sr clock with the maser, the lattice clock’s frequency can be calculated in the SI unit Hertz as realized by the Cs fountain clock. For white frequency noise, which is the dominating noise type in atomic frequency standards, the statistical clock uncertainty for a given averaging time  $\tau$  is equal to the Allan deviation  $u_{\text{clock}}(\tau) = \sigma_{\text{clock}}(\tau)$  [25]. Thus, the fountain clock’s instability  $\sigma_{\text{CSF2}}(\tau) = 1.7 \times 10^{-13} / \sqrt{\tau}$  clearly dominates the statistical uncertainty of the measurement given by  $u_A = \sqrt{\sigma_{\text{Sr}}^2(T_{\text{Sr}}) + \sigma_{\text{CSF2}}^2(T_{\text{Sr}})} = 3.3 \times 10^{-16}$ .

However, using only the joint uptimes of both clocks does not make any use of the information available from the maser: Its frequency is more stable than the fountain’s for periods of up

to  $10^5$  s and can be measured accurately even during short uptimes of the lattice clock. Therefore, it is reasonable to take the maser frequency value measured with the Sr clock as representative for longer intervals to improve  $u_A$ .

In general, due to the maser instability, there is a potential difference between the maser frequency averaged over time  $T_{\text{Sr}}$  and any chosen extended time  $T_{\text{ext}}$ . The lack of knowledge about this potential difference is expressed as an additional uncertainty  $u_{\text{ext}}$  which, given the knowledge of the maser flywheel's properties, can be calculated.

### 3. DATA ANALYSIS

The uncertainty  $u_{\text{ext}}$  arises from the extrapolation of the mean flywheel frequency measured with our Sr clock over time  $T_{\text{Sr}}$  to the longer time  $T_{\text{ext}}$ . With the help of Parseval's theorem,  $u_{\text{ext}}$  can be expressed by the flywheel's spectrum of frequency fluctuations  $S(f)$  and a weighting function  $g(t)$  that describes the respective measurement intervals (see Supplement 1).

The maser spectrum  $S(f)$  is extracted from different comparisons: the fast fluctuations and, thus, the stability at short averaging times  $\tau$  are obtained from a direct comparison with the Sr clock. The Allan deviation of a long continuous data set is presented in Fig. 2 (triangles). Mid- and low-frequency information about the maser's frequency fluctuations are obtained from preceding maser–maser comparisons (diamonds) and the measurements against the fountain clocks (dots, circles), respectively. From these data, we derive a model for  $S(f)$  that includes flicker frequency, white frequency, and flicker phase noise contributions. A linear maser drift was omitted here because the analysis was designed to be drift-insensitive (Supplement 1).

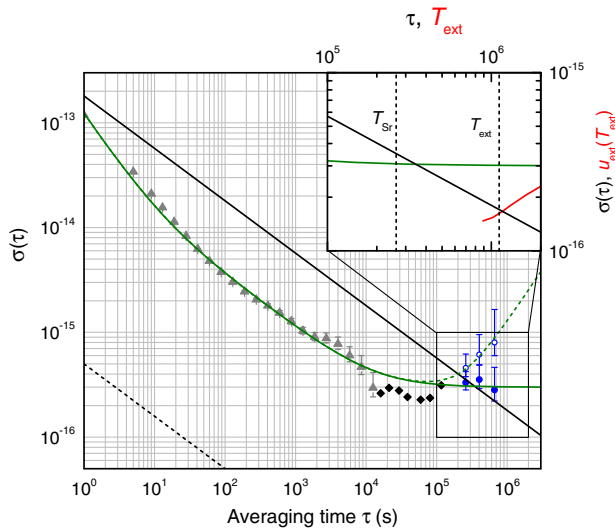


**Fig. 2.** Stability as represented by the Allan deviation  $\sigma$  of the relevant oscillators. Solid black line, fountain clock CSF2; dashed black line, Sr lattice clock; data points, measured maser stability (triangles: versus lattice clock; diamonds: maser comparisons; empty dots: against fountain clocks; filled dots: ditto without linear drift); solid (dashed) green line, noise model for the maser with (without) linear drift removed. The inset again shows the stabilities of the maser (green) and fountain clock (black). The red curve shows the additional uncertainty  $u_{\text{ext}}$  when the maser is used as a flywheel and data is extrapolated from an interval  $T_{\text{Sr}} = 267\,000$  s to  $T_{\text{ext}}$ . Dashed vertical lines indicate the direct and the optimum extrapolation measurement times.

The given Sr uptimes  $T_{\text{Sr}}$  [see Fig. 3(a)] and the length and distribution of the extended time  $T_{\text{ext}}$ , which we are free to choose, determine the weighting function  $g(t)$  [see Fig. 3(b) for the exemplary case of  $T_{\text{ext}} \approx 10^6$  s] and thus, together with  $S(f)$ , the corresponding extrapolation uncertainty  $u_{\text{ext}}$  (inset of Fig. 2). Due to the highly reliable Cs fountain, it was not necessary to consider the influence of its downtimes on  $g(t)$ .

For a flywheel-assisted Sr absolute frequency measurement, we optimize  $T_{\text{ext}}$  such that the overall statistical measurement uncertainty  $u_A = \sqrt{\sigma_{\text{Sr}}^2(T_{\text{Sr}}) + \sigma_{\text{CSF2}}^2(T_{\text{ext}}) + u_{\text{ext}}^2(T_{\text{ext}})}$  is minimized. As shown in the inset of Fig. 2, the extrapolation uncertainty reaches the statistical uncertainty of the primary clock CSF2 at about  $10^6$  s; further extension would degrade the combined statistical uncertainty  $u_A$ . We can therefore enlarge the data set from 267 000 s to about  $10^6$  s. In consequence, the fractional systematic uncertainty of the primary fountain clock of  $u_B(\text{CSF2}) = 3.1 \times 10^{-16}$  becomes the largest contribution to the overall uncertainty of this frequency measurement of our strontium lattice clock. The result for the Sr clock transition frequency is 429 228 004 229 872.97(16) Hz.

The evaluation procedure was applied accordingly to the later and longer measurement campaign with the Sr clock being operated from June 4 through 28 together with the same maser and both fountains: CSF1 ( $u_B(\text{CSF1}) = 3.0 \times 10^{-16}$ ) and CSF2 ( $u_B(\text{CSF2}) = 3.1 \times 10^{-16}$ ). The fountain clocks are considered independent (while the extrapolation and optical clock uncertainties are not) and the results have been suitably averaged, yielding

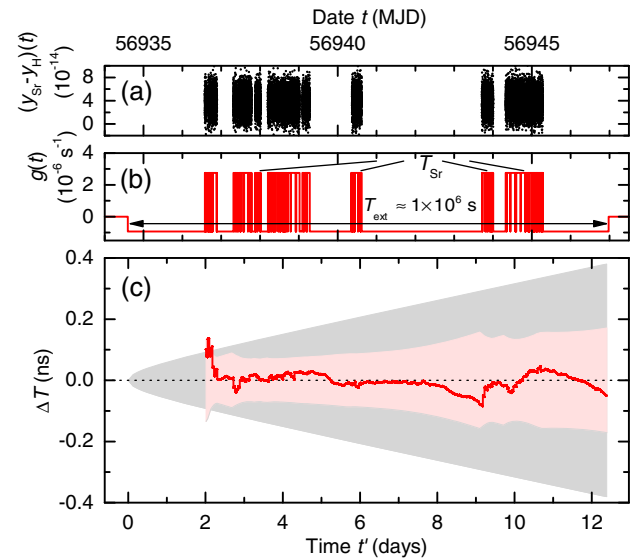


**Fig. 3.** Results achieved during measurement campaign 2014. (a) Frequency deviation between the nominal 100 MHz maser output and the Sr lattice clock averaged over 10 s assuming the Sr clock transition frequency is equal to the recommendation of the CIPM for the secondary representation of the “second” [26], in total 267 000 s. (b) Weighting function used to derive the calibration uncertainty of the hydrogen maser's frequency with respect to the Sr lattice clock for an interval of  $10^6$  s. (c) Estimated  $1\text{-}\sigma$  time uncertainty range of TS (Sr) (red shaded area) and TS(Cs) (gray shaded area) including statistical and systematic contributions. The red solid line depicts the time error of a simulated timescale realization TS(Sr) with respect to an ideal reference; it is shown starting with the first corrected interval [ $t' = 0$  corresponds to the Modified Julian Date (MJD)  $t \approx 56934.6$ ].

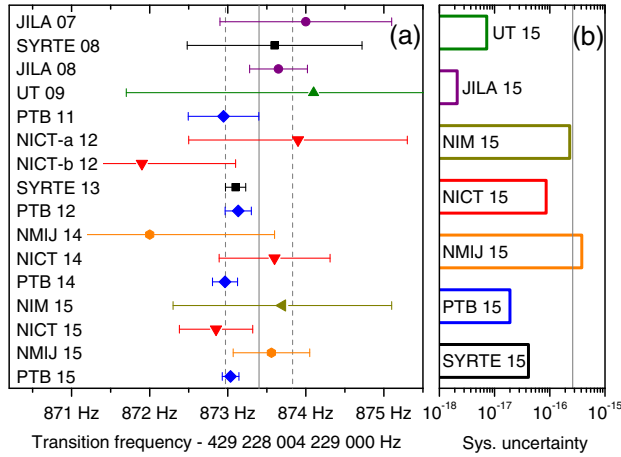


**Fig. 4.** (a) Comparison of measured absolute frequencies of the  $5s^2 \ ^1S_0 - 5s5p \ ^3P_0$  transition in  $^{87}\text{Sr}$ . The values have been obtained from various references [3,14,27–38]. PTB 14 and PTB 15 have been obtained in this work. The vertical line indicates the frequency recommended by the CIPM in 2013 for the secondary representation of the second by Sr lattice clocks [26]; the dashed lines show the assigned uncertainty. (b) Listing of the systematic uncertainty  $u_B$  of the best Sr clocks worldwide [9,36–40]. The gray line indicates the Cs systematic uncertainty of the absolute frequency measurement with the smallest overall uncertainty so far [3].

the Sr clock transition frequency of 429 228 004 229 873.04 (11) Hz. Due to the significantly longer measurement time, the overall statistical uncertainty is further improved and the use of two independent fountain clocks reduces the combined systematics.

Both measurements are in very good agreement with previous high-accuracy measurements [3,14] and provide a metrologically important confirmation that is necessary to build confidence in view of a redefinition of the SI unit “second.” The excellent agreement between absolute frequency measurements of strontium lattice clocks in numerous institutes is shown in Fig. 4(a). We want to emphasize that, due to the assistance of the flywheel, the achieved overall frequency measurement uncertainty in the 2015 campaign is the lowest one ever achieved. Figure 4(b) points out that the systematic uncertainties of present-day Sr clocks worldwide range from similar to well below the Cs systematics of the absolute frequency measurement with the lowest achieved uncertainty so far [3].

#### 4. REALIZING AN OPTICAL TIMESCALE

The combination of the intermittently operated but accurate Sr clock and the reliable but less accurate maser can as well be utilized to establish a continuous high-performance timescale TS(Sr) by steering the maser output frequency. This situation is not particular to optical clocks [37,38,41], but nowadays prevalent when timescales are established in metrology institutes or contributing to UTC [16,42–44].

In general, the steering algorithm can be optimized with respect to a stable scale unit or a good long-term performance. Both design goals coincide for 100% clock uptime, but they diverge the longer the clock downtimes are that must be bridged with a less-stable flywheel. For example, when the Sr clock

becomes available again after a long interruption, the flywheel instability may have led to a large time error. Thus, correcting the time error instantaneously will significantly distort the scale unit’s stability while the stability for longer averaging times is improved. For TS(Sr) we focus on a low statistical uncertainty for long averaging times. In order to provide time whenever needed, we choose a real-time implementation even though it can result in a degraded short-term stability compared to a post-processing approach.

The steering algorithm works as follows: The average maser frequency is calculated regularly once per hour using the frequency information available up to that point from the Sr clock. The average fractional frequency difference  $\overline{y_H - y_{Sr}}$  (see Supplement 1) is used as an estimate for the fractional maser frequency  $\tilde{y}_H$  over the full elapsed time  $t'$ . The corresponding time error  $\Delta T' = -t' \cdot \tilde{y}_H$  is applied to the phase stepper in Fig. 1 to correct the maser and yield TS(Sr). Please note that TS(Sr) is implemented by data post-processing. Since the realization procedure obeys causality, the procedure could have been implemented just as well in real-time. Moreover, more elaborate steering methods may be better suited for different scenarios, e.g., if other flywheels are considered.

The evaluation of the extrapolation uncertainty just discussed can be used to quantify the crucial parameter of the timescale—its predictability (or its uncertainty). The main difference from the situation of the absolute frequency measurement is that now we are not free to choose the extended time interval  $T_{\text{ext}}$  since it is determined by the timescale’s origin and the duration for which the timescale has to be provided. For convenience, we start with a discussion of an optical timescale that covers the 12 days of our first flywheel-assisted absolute frequency-measurement campaign.

The inset in Fig. 2 shows the frequency uncertainty  $u_{\text{ext}}(T_{\text{ext}})$  of an ensemble of masers—all having the same instability as our maser—whose frequencies are extrapolated from  $T_{\text{Sr}}$  to a continuous period  $T_{\text{ext}}$  (red line). The curve can be related to an accumulated timescale uncertainty via  $u_{\text{ext}}^{\text{TS}} = u_{\text{ext}}(T_{\text{ext}}) \cdot T_{\text{ext}}$  when realizing a timescale by correcting such maser’s frequency by intermittent measurements with our optical clock. To yield the overall optical timescale uncertainty, this contribution has to be added in quadrature to the accumulated time uncertainty of the Sr clock’s scale unit, which is at least an order of magnitude smaller. The uncertainty of TS(Sr) is compared to that of a theoretical timescale TS(Cs) based on a Cs reference with 100% uptime (assuming the parameters of PTB’s fountain clock CSF2).

Figure 3(c) shows 1- $\sigma$ -uncertainty bands of the timescales TS(Sr) and TS(Cs) as shaded areas including statistical and systematic contributions for the 2014 measurement campaign. In the case of TS(Sr), the statistical uncertainty connected to the interrupted optical clock operation  $u_{\text{ext}}^{\text{TS}}$  is calculated by the method just described, applying a weighting function that reflects the elapsed time and uptime of the optical clock. In this case,  $u_{\text{ext}}^{\text{TS}}$  is not insensitive to a linear drift of the flywheel for all times and thus an uncertainty contribution considering this fact is added in quadrature. However, in a real operation scenario the drift is usually known, e.g., from long-term comparisons against UTC, and can easily be corrected.

For the considered 12-day period, the uncertainty of TS(Sr) is well below 200 ps at all times. While the overall uncertainty of TS(Cs) is dominated by the reference clock’s systematics, that of TS(Sr) is governed by  $u_{\text{ext}}^{\text{TS}}$  due to its limited availability of the Sr clock of about 27%. Thus, with increasing optical clock

availability, the uncertainty of TS(Sr) would be further reduced. Yet, even with the optical clock-operation periods at hand, which can be considerably increased for the realization of a timescale, the uncertainty of TS(Sr) is clearly below that of the traditional timescale at all relevant times. Moreover, the uncertainty of TS(Cs) is increasing much faster.

To illustrate a typical behavior of TS(Sr) during the measurement interval of interest, we choose a numerical approach (see Supplement 1) since an experimental characterization requires an equal or even better reference timescale. A resulting TS(Sr) is given in Fig. 3(c), indicating its high stability. The initial transient response at day 2 is an artifact of the initialization of the real-time timescale and could be reduced considerably in post-processing. Between days six and nine, when no data from the lattice clock is available, TS(Sr) starts to deviate according to the free-running maser instability. From days six to eight, this effect is roughly compensated by the linear drift contribution. Once there is new optical data available ( $t > 9$  days) the time offset does not increase further and is even reduced due to an improved estimate of the past maser average frequency.

The approach just described was also applied to the maser-assisted Sr data acquired in 2015, where the Sr–maser comparison was performed not only for a longer time ( $T_{\text{Sr}} \approx 922\,000$  s) but also with a much higher overall availability of about 46% [see Fig. 5(a)]. This allows for a stable TS(Sr) over the extended period of 25 days, which is close to the typical 1-month reporting interval of UTC. The uncertainty bands of TS(Sr) compared to TS(Cs) are depicted in Fig. 5(b). The uncertainty of TS(Sr) is still governed by  $u_{\text{ext}}^{\text{TS}}$ , but the higher optical clock availability enables a timescale uncertainty of  $\lesssim 200$  ps for the whole 25-day period, which is a factor of 3.6 smaller than that of TS(Cs) that is controlled by an interruption-free CSF2. Thus, compared to the 2014 campaign, no larger timescale uncertainty was accumulated even though the timescale was provided for an interval of twice the length.

The agreement of the flywheel-assisted strontium absolute frequency measurement just presented and the conventional measurements [Fig. 4(a)] at the low  $10^{-16}$  level can be considered a confirmation of our uncertainty evaluation [a frequency

difference of  $3 \times 10^{-16}$  corresponds to a time error of  $\approx 300$  ps (650 ps) over 12 days (25 days)].

## 5. CONCLUSION

This paper demonstrates that optical frequency standards, and in particular strontium lattice clocks, have reached a maturity such that they now can be used in combination with a high-quality commercially available flywheel oscillator to generate a timescale that shows beyond state-of-the-art performance. This is essential for actual optical clock applications and a redefinition of the SI unit “second.” The measurement campaign presented in Fig. 3(a) did not explicitly aim for maximum uptime and can therefore be regarded a lower limit of capability of our apparatus. However, Fig. 3(c) shows that a time error of below 200 ps was achieved for a measurement interval of 12 days. In the second measurement campaign, a higher optical clock availability was realized yielding an improved time uncertainty of  $\lesssim 200$  ps over a 25-day interval, which is close to the typical comparison duration to establish UTC. This is a remarkably low value in view of the deviations in the ns range between the best timescales reported in the monthly Circular-T [45] which, however, includes an additional time-link error of about  $\lesssim 1$  ns.

Concerning the flywheel oscillator, several choices are available besides the H-maser used here to achieve lower scale-unit distortions for certain gap durations. Cryogenic sapphire microwave oscillators [46], cryogenic optical reference resonators [47–49], and lasers stabilized by the method of spectral hole burning [50] show excellent mid- and long-term stability and could serve this purpose. Even an optical clock that is optimized for reliability instead of accuracy can be envisaged. Ultimately, an ensemble of flywheels is conceivable, providing lowest instability for all occurring gap durations. For example, if we consider a flywheel with improved short-term stability by combining a laser stabilized to a state-of-the-art ultrastable reference cavity [19,48] with the reported maser following the approach of [51], the time deviation in the 2015 measurement campaign would be reduced by about 10%.

Today’s satellite-based comparison techniques can readily provide timescale comparisons with uncertainties below 1 ns [52]. Thus, having averaged for a year or more, the well-established satellite network would allow the intercontinental comparison of flywheel-assisted optical clocks in the low  $10^{-17}$  regime. Even further, ESA’s future space mission Atomic Clock Ensemble in Space will provide enhanced frequency comparison capabilities over intercontinental distances [53], such that flywheel-supported optical clock comparisons will no longer be limited by the satellite link between them. Thus, intercontinental clock comparisons with uncertainty in the  $10^{-18}$  regime after averaging over a month are within reach.

The current optical clocks can be developed toward mostly autonomous systems that will increase the average availabilities [54]. For example, a clock availability of 70% would immediately improve  $u_{\text{ext}}^{\text{TS}}$  further to below 60 ps over 30 days assuming our system and a worst-case scenario of a single 7 h interruption per day, which corresponds to a frequency uncertainty of  $2 \times 10^{-17}$ . Once optical clocks are engineered for maximum reliability, availabilities up to  $\geq 95\%$  may be achieved, which would result in an overall time error dominated by the systematics of our Sr lattice clock. However, optical clocks with even lower systematics have been reported recently [39,55], such that a time error of  $\leq 15$  ps per month could be achieved.

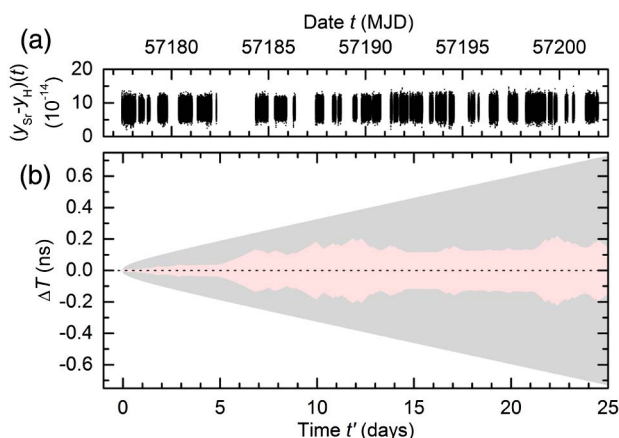


**Fig. 5.** Results achieved during measurement campaign 2015. (a) Frequency deviation between maser and the Sr clock. (b)  $1\text{-}\sigma$  time uncertainty range of TS(Sr) (red) and TS(Cs) (gray), including statistical and systematic contributions.

**Funding.** Centre of Quantum Engineering and Space-Time Research (QUEST); German Research Foundation (DFG) (RTG 1729, CRC 1128); International Timescales with Optical Clocks (ITOC).

**Acknowledgment.** We gratefully acknowledge Andreas Bauch for helpful discussions. ITOC is part of the European Metrology Research Programme (EMRP), which is jointly funded by the EMRP participating countries within EURAMET and the European Union.

See Supplement 1 for supporting content.

## REFERENCES

1. "On the future revision of the SI," 2014, <http://www.bipm.org/en/measurement-units/new-si/>.
2. C. W. Chou, D. B. Hume, J. C. J. Koelemeij, D. J. Wineland, and T. Rosenband, "Frequency comparison of two high-accuracy Al<sup>+</sup> optical clocks," *Phys. Rev. Lett.* **104**, 070802 (2010).
3. R. Le Targat, L. Lorini, Y. Le Coq, M. Zawada, J. Guéna, M. Abgrall, M. Gurov, P. Rosenbusch, D. G. Rovera, B. Nagórny, R. Gartman, P. G. Westergaard, M. E. Tobar, M. Lours, G. Santarelli, A. Clairon, S. Bize, P. Laurent, P. Lemonde, and J. Lodewyck, "Experimental realization of an optical second with strontium lattice clocks," *Nat. Commun.* **4**, 2109 (2013).
4. P. Dubé, A. A. Madej, Z. Zhou, and J. E. Bernard, "Evaluation of systematic shifts of the <sup>86</sup>Sr<sup>+</sup> single-ion optical frequency standard at the 10<sup>-17</sup> level," *Phys. Rev. A* **87**, 023806 (2013).
5. N. Hinkley, J. A. Sherman, N. B. Phillips, M. Schioppa, N. D. Lemke, K. Beloy, M. Pizzocaro, C. W. Oates, and A. D. Ludlow, "An atomic clock with 10<sup>-18</sup> instability," *Science* **341**, 1215–1218 (2013).
6. B. J. Bloom, T. L. Nicholson, J. R. Williams, S. L. Campbell, M. Bishof, X. Zhang, W. Zhang, S. L. Bromley, and J. Ye, "An optical lattice clock with accuracy and stability at the 10<sup>-18</sup> level," *Nature* **506**, 71–75 (2014).
7. N. Huntemann, B. Lipphardt, C. Tamm, V. Gerginov, S. Weyers, and E. Peik, "Improved limit on a temporal variation of  $m_p/m_e$  from comparisons of Yb<sup>+</sup> and Cs atomic clocks," *Phys. Rev. Lett.* **113**, 210802 (2014).
8. R. M. Godun, P. B. R. Nisbet-Jones, J. M. Jones, S. A. King, L. A. M. Johnson, H. S. Margolis, K. Szymaniec, S. N. Lea, K. Bongs, and P. Gill, "Frequency ratio of two optical clock transitions in <sup>171</sup>Yb<sup>+</sup> and constraints on the time-variation of fundamental constants," *Phys. Rev. Lett.* **113**, 210801 (2014).
9. I. Ushijima, M. Takamoto, M. Das, T. Ohkubo, and H. Katori, "Cryogenic optical lattice clocks," *Nat. Photonics* **9**, 185–189 (2015).
10. A. D. Ludlow, M. M. Boyd, J. Ye, E. Peik, and P. O. Schmidt, "Optical atomic clocks," *Rev. Mod. Phys.* **87**, 637–701 (2015).
11. F. Riehle, "Towards a redefinition of the second based on optical atomic clocks," *C.R. Physique* **16**, 506–515 (2015), Special Issue on The Measurement of Time/La Mesure Du Temps.
12. H. Margolis, "Timekeepers of the future," *Nat. Phys.* **10**, 82–83 (2014).
13. P. Gill and F. Riehle, "On secondary representations of the second," in *Proceedings of the 2006 Meeting of the European Frequency and Time Forum*, Braunschweig, 2006, pp. 282–288.
14. S. Falke, N. Lemke, C. Grebing, B. Lipphardt, S. Weyers, V. Gerginov, N. Huntemann, C. Hagemann, A. Al-Masoudi, S. Häfner, S. Vogt, U. Sterr, and C. Lisdat, "A strontium lattice clock with 3 × 10<sup>-17</sup> inaccuracy and its frequency," *New J. Phys.* **16**, 073023 (2014).
15. G. Petit, F. Arias, A. Harnegnies, G. Panfilo, and L. Tisserand, "UTC<sub>r</sub>: a rapid realization of UTC," *Metrologia* **51**, 33–39 (2014).
16. T. E. Parker, "Invited review article: the uncertainty in the realization and dissemination of the SI second from a systems point of view," *Rev. Sci. Instrum.* **83**, 021102 (2012).
17. A. Bauch, S. Weyers, D. Piester, E. Staliuniene, and W. Yang, "Generation of UTC(PTB) as a fountain-clock based time scale," *Metrologia* **49**, 180–188 (2012).
18. Ł. Śliwaczyński, P. Krehlik, A. Czubla, Ł. Buczek, and M. Lipiński, "Dissemination of time and RF frequency via a stabilized fibre optic link over a distance of 420 km," *Metrologia* **50**, 133–145 (2013).
19. S. Häfner, S. Falke, C. Grebing, S. Vogt, T. Legero, M. Merimaa, C. Lisdat, and U. Sterr, "8 × 10<sup>-17</sup> fractional laser frequency instability with a long room-temperature cavity," *Opt. Lett.* **40**, 2112–2115 (2015).
20. A. Al-Masoudi, S. Dörscher, S. Häfner, U. Sterr, and C. Lisdat, "Noise and instability of an optical lattice clock," *Phys. Rev. A* **92**, 063814 (2015).
21. S. Weyers, U. Hübner, R. Schröder, C. Tamm, and A. Bauch, "Uncertainty evaluation of the atomic caesium fountain CSF1 of the PTB," *Metrologia* **38**, 343–352 (2001).
22. S. Weyers, A. Bauch, R. Schröder, and C. Tamm, "The atomic caesium fountain CSF1 of PTB," in *Frequency Standards and Metrology, Proceedings of the Sixth Symposium*, P. Gill, ed. (World Scientific, 2002), pp. 64–71.
23. V. Gerginov, N. Nemitz, S. Weyers, R. Schröder, R. D. Griebisch, and R. Wynands, "Uncertainty evaluation of the caesium fountain clock PTB-CSF2," *Metrologia* **47**, 65–79 (2010).
24. S. Weyers, V. Gerginov, N. Nemitz, R. Li, and K. Gibble, "Distributed cavity phase frequency shifts of the caesium fountain PTB-CSF2," *Metrologia* **49**, 82–87 (2012).
25. E. Benkler, C. Lisdat, and U. Sterr, "On the relation between uncertainties of weighted frequency averages and the various types of Allan deviations," *Metrologia* **52**, 565–574 (2015).
26. BIPM, *Report of the 101th meeting of the Comité International des Poids et Mesures (CIPM)* (Bureau International des Poids et Mesures (BIPM), 2013).
27. M. M. Boyd, A. D. Ludlow, S. Blatt, S. M. Foreman, T. Ido, T. Zelevinsky, and J. Ye, "<sup>87</sup>Sr lattice clock with inaccuracy below 10<sup>-15</sup>," *Phys. Rev. Lett.* **98**, 083002 (2007).
28. X. Baillard, M. Fouché, R. L. Targat, P. G. Westergaard, A. Lecallier, F. Chapelet, M. Abgrall, G. D. Rovera, P. Laurent, P. Rosenbusch, S. Bize, G. Santarelli, A. Clairon, P. Lemonde, G. Grosche, B. Lipphardt, and H. Schnatz, "An optical lattice clock with spin-polarized <sup>87</sup>Sr atoms," *Eur. Phys. J. D* **48**, 11–17 (2008).
29. G. K. Campbell, A. D. Ludlow, S. Blatt, J. W. Thomsen, M. J. Martin, M. H. G. de Miranda, T. Zelevinsky, M. M. Boyd, J. Ye, S. A. Diddams, T. P. Heavner, T. E. Parker, and S. R. Jefferts, "The absolute frequency of the <sup>87</sup>Sr optical clock transition," *Metrologia* **45**, 539–548 (2008).
30. F.-L. Hong, M. Musha, M. Takamoto, H. Inaba, S. Yanagimachi, A. Takamizawa, K. Watabe, T. Ikegami, M. Imae, Y. Fujii, M. Amemiya, K. Nakagawa, K. Ueda, and H. Katori, "Measuring the frequency of a Sr optical lattice clock using a 120 km coherent optical transfer," *Opt. Lett.* **34**, 692–694 (2009).
31. S. Falke, H. Schnatz, J. S. R. Vellore Winfred, T. Middelman, S. Vogt, S. Weyers, B. Lipphardt, G. Grosche, F. Riehle, U. Sterr, and C. Lisdat, "The <sup>87</sup>Sr optical frequency standard at PTB," *Metrologia* **48**, 399–407 (2011).
32. A. Yamaguchi, N. Shiga, S. Nagano, Y. Li, H. Ishijima, H. Hachisu, M. Kumagai, and T. Ido, "Stability transfer between two clock lasers operating at different wavelengths for absolute frequency measurement of clock transition in <sup>87</sup>Sr," *Appl. Phys. Express* **5**, 022701 (2012).
33. K. Matsubara, H. Hachisu, Y. Li, S. Nagano, C. Locke, A. Nohgami, M. Kajita, K. Hayasaka, T. Ido, and M. Hosokawa, "Direct comparison of a Ca<sup>+</sup> single-ion clock against a Sr lattice clock to verify the absolute frequency measurement," *Opt. Express* **20**, 22034–22041 (2012).
34. D. Akamatsu, H. Inaba, K. Hosaka, M. Yasuda, A. Onae, T. Suzuyama, M. Amemiya, and F.-L. Hong, "Spectroscopy and frequency measurement of the <sup>87</sup>Sr clock transition by laser linewidth transfer using an optical frequency comb," *Appl. Phys. Express* **7**, 012401 (2014).
35. H. Hachisu, M. Fujieda, S. Nagano, T. Gotoh, A. Nogami, T. Ido, S. Falke, N. Huntemann, C. Grebing, B. Lipphardt, C. Lisdat, and D. Piester, "Direct comparison of optical lattice clocks with an intercontinental baseline of 9000 km," *Opt. Lett.* **39**, 4072–4075 (2014).
36. Y.-G. Lin, Q. Wang, Y. Li, F. Meng, B.-K. Lin, E.-J. Zang, Z. Sun, F. Fang, T.-C. Li, and Z.-J. Fang, "First evaluation and frequency measurement of the strontium optical lattice clock at NIM," *Chin. Phys. Lett.* **32**, 090601 (2015).
37. H. Hachisu and T. Ido, "Intermittent optical frequency measurements to reduce the dead time uncertainty of frequency link," *Jpn. J. Appl. Phys.* **54**, 112401 (2015).
38. T. Tanabe, D. Akamatsu, T. Kobayashi, A. Takamizawa, S. Yanagimachi, T. Ikegami, T. Suzuyama, H. Inaba, S. Okubo, M. Yasuda, F.-L. Hong, A. Onae, and K. Hosaka, "Improved frequency measurement of the <sup>1</sup>S<sub>0</sub>-<sup>3</sup>P<sub>0</sub> clock transition in <sup>87</sup>Sr using a Cs fountain clock as a transfer oscillator," *J. Phys. Soc. Jpn.* **84**, 115002 (2015).

39. T. L. Nicholson, S. L. Campbell, R. B. Hutson, G. E. Marti, B. J. Bloom, R. L. McNally, W. Zhang, M. D. Barrett, M. S. Safronova, G. F. Strouse, W. L. Tew, and J. Ye, "Systematic evaluation of an atomic clock at  $2 \times 10^{-18}$  total uncertainty," *Nat. Commun.* **6**, 6896 (2015).
40. C. Lisdat, G. Grosche, N. Quintin, C. Shi, S. M. F. Raupach, C. Grebing, D. Nicolodi, F. Stefani, A. Al-Masoudi, S. Dörscher, S. Häfner, J. L. Robyr, N. Chiodo, S. Bilicki, E. Bookjans, A. Koczwara, S. Koke, A. Kuhl, F. Wiotte, F. Meynadier, E. Camisard, M. Abgrall, M. Lours, T. Legero, H. Schnatz, U. Sterr, H. Denker, C. Chardonnet, Y. Le Coq, G. Santarelli, A. Amy-Klein, R. Le Targat, J. Lodewyck, O. Lopez, and P.-E. Pottie, "A clock network for geodesy and fundamental science," arXiv:1511.07735v1 (2015).
41. J. Leute, N. Huntemann, B. Lipphardt, C. Tamm, P. B. R. Nisbet-Jones, S. A. King, R. M. Godun, J. M. Jones, H. S. Margolis, P. B. Whibberley, A. Wallin, M. Merimaa, P. Gill, and E. Peik, "Frequency comparison of  $^{171}\text{Yb}^+$  ion optical clocks at PTB and NPL via GPS PPP," arXiv:1507.04754v1 (2015).
42. J. Levine, "Invited review article: the statistical modeling of atomic clocks and the design of time scales," *Rev. Sci. Instrum.* **83**, 021101 (2012).
43. D.-H. Yu, M. Weiss, and T. E. Parker, "Uncertainty of a frequency comparison with distributed dead time and measurement interval offset," *Metrologia* **44**, 91–96 (2007).
44. R. J. Douglas and J.-S. Boulanger, "Standard uncertainty for average frequency traceability," in *Proceedings of the 11th European Frequency and Time Forum (EFTF)*, Neuchâtel, Switzerland, March 4–7, 1997, pp. 345–349.
45. "BIPM CircularT," <http://www.bipm.org/jsp/en/TimeFtp.jsp>.
46. J. G. Hartnett, N. R. Nand, and C. Lu, "Ultra-low-phase-noise cryocooled microwave dielectric-sapphire-resonator oscillators," *Appl. Phys. Lett.* **100**, 183501 (2012).
47. R. Storz, C. Braxmaier, K. Jäck, O. Pradl, and S. Schiller, "Ultrahigh long-term dimensional stability of a sapphire cryogenic optical resonator," *Opt. Lett.* **23**, 1031–1033 (1998).
48. T. Kessler, C. Hagemann, C. Grebing, T. Legero, U. Sterr, F. Riehle, M. J. Martin, L. Chen, and J. Ye, "A sub-40-mHz-linewidth laser based on a silicon single-crystal optical cavity," *Nat. Photonics* **6**, 687–692 (2012).
49. C. Hagemann, C. Grebing, C. Lisdat, S. Falke, T. Legero, U. Sterr, F. Riehle, M. J. Martin, and J. Ye, "Ultra-stable laser with average fractional frequency drift rate below  $5 \times 10^{-19}/\text{s}$ ," *Opt. Lett.* **39**, 5102–5105 (2014).
50. M. J. Thorpe, L. Rippe, T. M. Fortier, M. S. Kirchner, and T. Rosenband, "Frequency-stabilization to  $6 \times 10^{-16}$  via spectral-hole burning," *Nat. Photonics* **5**, 688–693 (2011).
51. S. M. F. Raupach, T. Legero, C. Grebing, C. Hagemann, T. Kessler, A. Koczwara, B. Lipphardt, M. Misera, H. Schnatz, G. Grosche, and U. Sterr, "Subhertz-linewidth infrared frequency source with a long-term instability below  $5 \times 10^{-15}$ ," *Appl. Phys. B* **110**, 465–470 (2013).
52. G. Panfilo and T. E. Parker, "A theoretical and experimental analysis of frequency transfer uncertainty, including frequency transfer into TAI," *Metrologia* **47**, 552–560 (2010).
53. L. Cacciapuoti and C. Salomon, "Space clocks and fundamental tests: the ACES experiment," *Eur. Phys. J. Spec. Top.* **172**, 57–68 (2009).
54. G. P. Barwood, P. Gill, G. Huang, and H. A. Klein, "Automatic laser control for a  $^{88}\text{Sr}^+$  optical frequency standard," *Meas. Sci. Technol.* **23**, 055201 (2012).
55. N. Huntemann, C. Sanner, B. Lipphardt, C. Tamm, and E. Peik, "Single-ion atomic clock with  $3 \times 10^{-18}$  systematic uncertainty," *Phys. Rev. Lett.* **116**, 063001 (2016).